

Origin of tradeoff between movement velocity and attachment duration of kinesin motor on a microtubule

Yuying Liu(刘玉颖) and Zhiqiang Zhang(张志强)

Citation: Chin. Phys. B, 2024, 33 (**2**): 028708. DOI: 10.1088/1674-1056/ad1177
Journal homepage: http://cpb.iphy.ac.cn; http://iopscience.iop.org/cpb

What follows is a list of articles you may be interested in

Regulation of the intermittent release of giant unilamellar vesicles under osmotic pressure

Qi Zhou(周琪), Ping Wang(王平), Bei-Bei Ma(马贝贝), Zhong-Ying Jiang(蒋中英), and Tao Zhu(朱涛)
Chin. Phys. B, 2022, 31 (**9**): 098701. DOI: 10.1088/1674-1056/ac4a69

An electromagnetic view of relay time in propagation of neural signals

Jing-Jing Xu(徐晶晶), San-Jin Xu(徐三津), Fan Wang(王帆), and Sheng-Yong Xu(许胜勇)
Chin. Phys. B, 2021, 30 (**2**): 028701. DOI: 10.1088/1674-1056/abc0d2

Mechanochemical model for myosin II dimer that can explain the spontaneous oscillatory contraction of muscle

Wei Sun(孙伟), Xiao-Yang Zhao(赵晓阳), Jun-Ping Zhang(张俊萍), Tala(塔拉), Wei-Sheng Guo(郭维生)
Chin. Phys. B, 2018, 27 (**11**): 118702. DOI: 10.1088/1674-1056/27/11/118702

Molecular modeling of oscillating GHz electric field influence on the kinesin affinity to microtubule

H. R. Saeidi, S. S. Setayandeh, A. Lohrasebi
Chin. Phys. B, 2015, 24 (**8**): 080701. DOI: 10.1088/1674-1056/24/8/080701

Propagation of kink-antikink pair along microtubules as a control mechanism for polymerization and depolymerization processes

L. Kavitha, A. Muniyappan, S. Zdravković, M. V. Satarić, A. Marlewski, S. Dhamayanthi, D. Gopi
Chin. Phys. B, 2014, 23 (**9**): 098703. DOI: 10.1088/1674-1056/23/9/098703

Origin of tradeoff between movement velocity and attachment duration of kinesin motor on a microtubule

Yuying Liu(刘玉颖)[1,†] and Zhiqiang Zhang(张志强)[2]

[1] *Department of Physics, College of Science, China Agricultural University, Beijing* 100083, *China*
[2] *Basic Ministry, Space Engineering University, Beijing* 101416, *China*

(Received 30 September 2023; revised manuscript received 16 November 2023; accepted manuscript online 1 December 2023)

Kinesin-1 motor protein is a homodimer containing two identical motor domains connected by a common long coiled-coil stalk via two flexible neck linkers. The motor can step on a microtubule with a velocity of about 1 μm·s^{-1} and an attachment duration of about 1 s under physiological conditions. The available experimental data indicate a tradeoff between velocity and attachment duration under various experimental conditions, such as variation of the solution temperature, variation of the strain between the two motor domains, and so on. However, the underlying mechanism of the tradeoff is unknown. Here, the mechanism is explained by a theoretical study of the dynamics of the motor under various experimental conditions, reproducing quantitatively the available experimental data and providing additional predictions. How the various experimental conditions lead to different decreasing rates of attachment duration versus velocity is also explained.

Keywords: motor protein, velocity, detachment time, processivity

PACS: 87.10.Tf, 87.15.A–, 87.15.hg **DOI:** 10.1088/1674-1056/ad1177

1. Introduction

Kinesin-1 motor proteins were first discovered as members of the kinesin superfamily.[1,2] Since the discovery of kinesin-1 proteins, their structures and dynamics have been thoroughly studied.[3–11] The kinesin-1 motor is a homodimer containing two identical motor domains (or heads) connected by a common long coiled-coil stalk via two flexible neck linkers (NLs).[3,12] The dimeric motor can walk hand-over-hand on a microtubule (MT) filament towards the plus end with a velocity of about 1 μm·s^{-1} and a run length of about 1 μm before detachment under physiological conditions, performing the function of intracellular transport.[13–15] The directional motion of the motor is powered by the hydrolysis of ATP molecules, with about one ATP molecule consumed per mechanical step of about 8.2 nm under the unloaded case.[14–18] Since in this work we focus only on the kinesin-1 motor, for convenience it is simply called the kinesin motor.

Apart from wild-type (WT) kinesin motors under physiological conditions, the dynamics of WT kinesin motors under non-physiological conditions and mutant or engineered kinesin motors under physiological conditions have also been studied experimentally in detail.[19–25] For example, Nara and Ishiwata[25] studied the dynamics of the bovine brain kinesin motor in the solution temperature range 20 °C–40 °C. Interestingly, they found that both the velocity and run length of the motor increased with increase in temperature, while the duration of the motor attaching to an MT decreased with increase in temperature. Yildiz *et al.*[21] studied the dynamics of engineered human kinesin motors with different numbers of residues inserted between the NLs and the coiled-coil stalk. Puzzlingly, they found that with an increase in the number of inserted residues, implying a decrease in the strain between the two heads in the two-head bound state, the velocity and chemomechanical coupling ratio (defined as the number of mechanical steps per ATP molecule consumed) of the motor decreased. By contrast, insertion had nearly no effect on the ATPase rate, and with an increase in the number of inserted residues the run length decreased only slightly. Both the experimental data of Nara and Ishiwata[25] and those of Yildiz *et al.*[21] indicated that the attachment duration (T_a) of the motor on a MT decreases with increase in the velocity (v), implying a tradeoff between the two factors. As noted recently by Rizvi,[26] the experimental data on the relationship between the two factors can be approximately fitted by a power-law relation, $T_a \propto v^{-\alpha}$, with its exponent $\alpha > 0$ under the variation of temperature being smaller than that under the variation of intramolecular strain.

However, the underlying mechanism of these features in the relationship between velocity and attachment duration is unclear. In this work, we address this issue. For this purpose, we study theoretically the dynamics of the motor under variation of intramolecular strain, solution temperature, ATP concentration and rate of ATP transition to ADP that can be realized by mutating the residues near the nucleotide-binding pocket, reproducing quantitatively the available experimental data and providing predicted results.

[†]Corresponding author. E-mail: liuyuying@cau.edu.cn

© 2024 Chinese Physical Society and IOP Publishing Ltd

2. General equations for the dynamics of the kinesin motor

To study the tradeoff between velocity and attachment duration of the kinesin motor, we use the model for chemomechanical coupling of the kinesin motor proposed by Xie,[27] which gives a good explanation of diverse experimental data on the dynamics of the motor.[9–11,27–30] The pathway of the chemomechanical coupling at saturating ATP concentrations is schematically shown in Fig. 1, and has been described in detail before[27] (see also supplementary information). Throughout we focus on the case of no load on the motor. Before NL docking, the NL of the MT-bound head is not in the forward orientation under no load on the coiled-coil stalk (Fig. 1(b)), so the rate of ATP transition to ADP is much smaller than the NL-docking rate; thus, for simplicity, the transition of ATP to ADP in the MT-bound head before NL docking in Fig. 1(b) is not considered here.

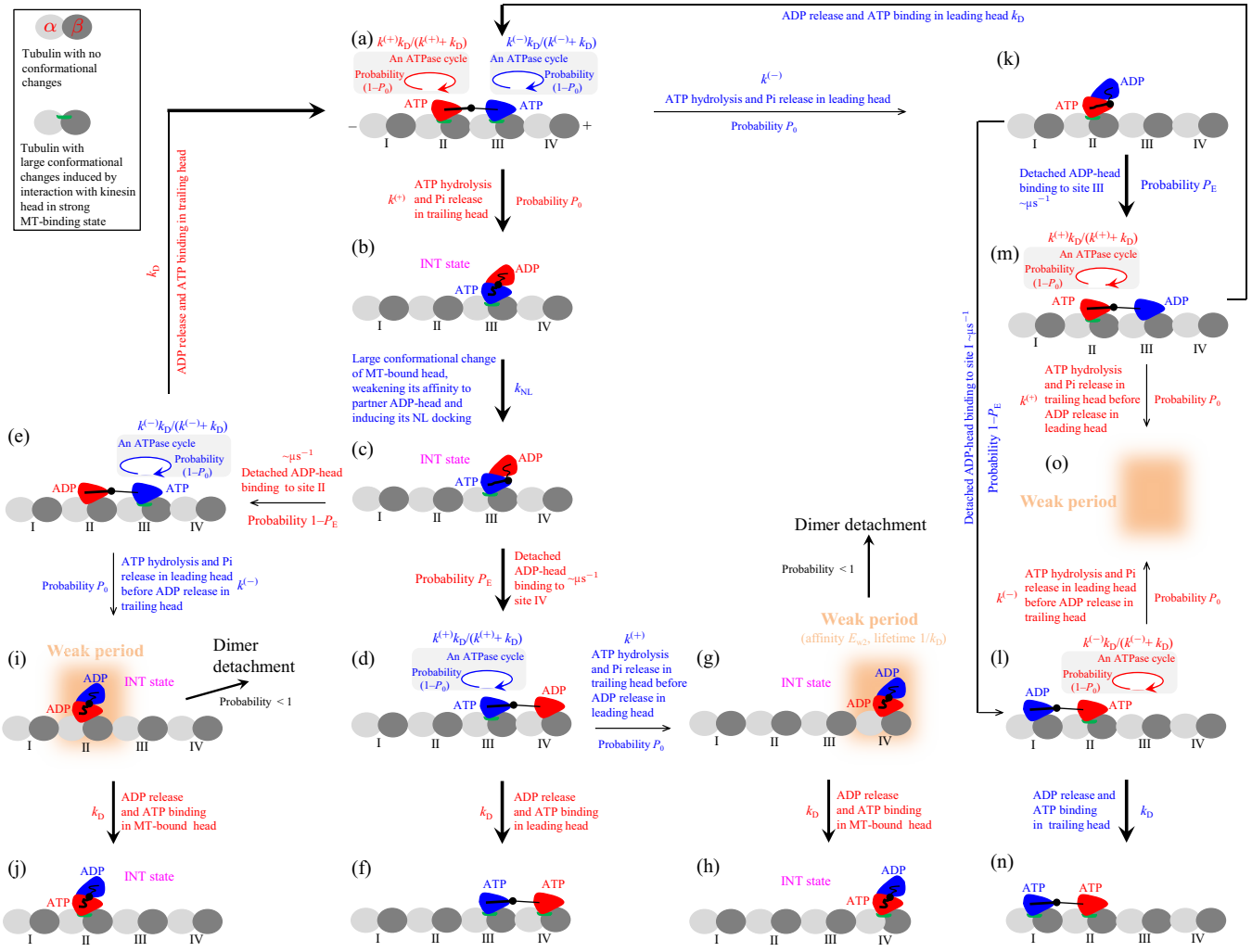


Fig. 1. Model of kinesin dimer stepping on and detachment from MT. Panels (a)–(o) illustrate the chemomechanical coupling pathway at saturating ATP concentrations (see supplementary information for a detailed description). The figure is modified from that in Refs. [27,28].

Based on Fig. 1, the equations for the dynamics of the motor at saturating ATP concentrations are briefly presented in the following.

In the intermediate (INT) state, after the reduction of the binding energy between the two heads (Fig. 1(c)), the probability P_E for the detached head to diffuse forward and to bind to the front tubulin can be written as[27]

$$P_E = \frac{\exp\left(\frac{E_0}{k_B T}\right)}{\exp\left(\frac{E_0}{k_B T}\right)+1}, \tag{1}$$

where E_0 is the total free energy change associated with the large conformational change of the head in the ATP state and the NL docking, k_B is the Boltzmann constant and T is the absolute temperature. In this work, we focus only on the case of no load on the motor. Under a load, P_E is a function of the load.[27]

In the two-head bound state (Fig. 1(a)), after ATP transition to ADP in one head, by overcoming the weak affinity E_{w1} of the head for local $\alpha\beta$-tubulin within a short time t_r (of the order of 10 μs), the probability for the ADP head to detach from the local tubulin and then diffuse to the INT position is denoted by P_0. The rates of transition of ATP to ADP

in the head with the forward NL orientation and that without the forward NL orientation are denoted by $k^{(+)}$ and $k^{(-)}$, respectively. The rate of ADP release from the head bound to MT is denoted by $k_{\rm D}$, which is considered here to be independent of NL orientation. In the INT state (Fig. 1(b)), the rate of the large conformational change of the ATP head, which is associated with NL docking and great reduction in the binding energy between the two heads, is denoted by $k_{\rm NL}$. During the stepping process, the average ATPase rates of the trailing and leading heads, which are denoted by $k_{\rm T}$ and $k_{\rm L}$, respectively, can be approximately written as[27]

$$k_{\rm T}=\left(\frac{1}{k_{\rm D}}+\frac{1}{k^{(+)}}\right)^{-1}(1-P_0)+\left(\frac{1}{k^{(+)}}+\frac{1}{k_{\rm NL}}\right)^{-1}P_0P_{\rm E}+\left(\frac{1}{k_{\rm D}}+\frac{1}{k^{(+)}}+\frac{1}{k_{\rm NL}}\right)^{-1}P_0\left(1-P_{\rm E}\right), \tag{2}$$

$$k_{\rm L}=\left(\frac{1}{k_{\rm D}}+\frac{1}{k^{(-)}}\right)^{-1}(1-P_0)+\left(\frac{1}{k_{\rm D}}+\frac{1}{k^{(-)}}\right)^{-1}P_0P_{\rm E}+k^{(-)}P_0\left(1-P_{\rm E}\right). \tag{3}$$

The total ATPase rate of the motor can be written as

$$k=k_{\rm T}+k_{\rm L}. \tag{4}$$

The velocity of the motor can be written as[27]

$$v=\left[P_0P_{\rm E}k_{\rm T}-P_0\left(1-P_{\rm E}\right)k_{\rm L}\right]d, \tag{5}$$

where $d=8.2$ nm is the step size (the periodicity of the MT filament). The chemomechanical coupling ratio can be written as

$$R=\frac{v}{kd}. \tag{6}$$

In the weak MT-binding period (Figs. 1(g), 1(i), and 1(o)), both heads are in the ADP state, with one head bound to MT with affinity $E_{\rm w2}$ ($>E_{\rm w1}$) and the other detached from MT having a high binding energy to the MT-bound head. The occurrence probability of the weak MT-binding period in one ATPase cycle can be written as[27]

$$P_{\rm w}=P_0P_{\rm E}\frac{k^{(+)}}{k^{(+)}+k_{\rm D}}+P_0\left(1-P_{\rm E}\right)\frac{k^{(-)}}{k^{(-)}+k_{\rm D}}. \tag{7}$$

The detachment probability of the motor during the weak MT-binding period can be written as[27]

$$P_{\rm d}=\frac{k_{\rm d}}{k_{\rm d}+k_{\rm D}}, \tag{8}$$

where $k_{\rm d}$ is the detachment rate during the weak MT-binding period. The detachment rate of the motor during processive motion, which arises from detachment occurring in the weak MT-binding period, can be written as[27]

$$\varepsilon_{\rm w}=\left(k_{\rm T}+k_{\rm L}\right)P_{\rm w}P_{\rm d}. \tag{9}$$

During processive motion of the motor, the weak MT-binding period can only occur occasionally in one chemomechanical coupling cycle, and if it occurs it constitutes only a small fraction of the whole period of the chemomechanical coupling cycle because ADP release is a non-limiting step of ATPase activity. This implies that in one chemomechanical coupling cycle the motor is almost always in the strong MT-binding period. Denoting the detachment rate of the motor during the strong MT-binding period by $\varepsilon_{\rm s}$, the total detachment rate of the motor can then be approximately written as[29]

$$\varepsilon=\varepsilon_{\rm w}+\varepsilon_{\rm s}. \tag{10}$$

The duration of the motor attaching to MT can then be calculated with

$$T_{\rm a}=\frac{1}{\varepsilon}. \tag{11}$$

The run length can then be calculated with

$$L=\frac{v}{\varepsilon}. \tag{12}$$

3. Results and discussion

In a previous work,[27] the load dependences of the velocity, run length and dissociation rate of WT kinesin motors were studied. In this work, in order to explore the physical origin of the tradeoff between the velocity and total attachment duration of the kinesin motor on MT we study the effects of varying intramolecular strain, solution temperature, ATP concentration and the rate of ATP transition to ADP on the velocity and attachment duration.

3.1. Effect of varying intramolecular strain

In this section, we study the effect of varying intramolecular strain on the dynamics of a human kinesin motor at saturating ATP concentrations. As in the experiments of Yildiz *et al.*,[21] variation of intramolecular strain can be realized by inserting additional residues with various lengths of polyproline and glycine–serine repeats, preceded by two lysines and followed by a single glycine residue, between the NL and the coiled-coil stalk. As in Ref. [21], the engineered dimer with the insertion of n prolines is called nP, where n is an integer, and the engineered dimer with the insertion of seven repeats of glycine–serine residues is called 14GS. The engineered NL of 14GS is more flexible than that of 26P.[21] As previous all-atom molecular dynamics simulations showed,[30] for the WT dimer with each NL having 14 residues a large intramolecular strain of about 28 pN can be induced when the two heads are bound to two successive tubulins on an MT filament, which are 8.2 nm apart. As noted in Ref. [21], the engineered nP dimer has a smaller intramolecular strain than the WT dimer; with increase in n the intramolecular strain becomes smaller, and the engineered 14GS dimer has a smaller intramolecular

strain than the 26P dimer. As shown by previous Brownian dynamics simulations,[30] for the WT dimer after ATP transition to ADP in one head the large intramolecular strain can easily drive the ADP head to detach from the local tubulin and diffuse to the INT position with probability $P_0 \approx 1$, whereas for the engineered dimer with the insertion of six residues in the NL, due to the smaller intramolecular strain P_0 becomes evidently smaller than 1. Moreover, it is expected that P_0 decreases with increase in n for the nP dimers, and the 14GS dimer has a smaller P_0 than the 26P dimer.

As seen from Eqs. (1)–(12), to study theoretically the dynamics of the WT and engineered motors, values for the parameters $k^{(+)}$, $k^{(-)}$, $k_{\rm D}$, $k_{\rm NL}$, E_0, $k_{\rm d}$, $\varepsilon_{\rm s}$ and P_0 are required. Here, for human kinesin under the experimental conditions of Yildiz *et al.*[21] we take $k^{(-)} = 3.6\ {\rm s}^{-1}$, $k_{\rm D} = 300\ {\rm s}^{-1}$, $k_{\rm NL} = 1500\ {\rm s}^{-1}$ and $E_0 = 3.6 k_{\rm B}T$ (Table 1), which are the same as those determined previously that quantitatively explain the available experimental data for Drosophila kinesin.[27] In addition, we take $\varepsilon_{\rm s}$to be very small, for example $\varepsilon_{\rm s} = 0.01\ {\rm s}^{-1}$ (Table 1), which quantitatively explains the available experimental data.[9] The other three parameters $k^{(+)}$, $k_{\rm d}$ and P_0 are adjustable here to make the theoretical results consistent with the experimental data of Yildiz *et al.*[21] By taking $k^{(+)} = 62\ {\rm s}^{-1}$ (Table 1), the theoretical results for velocity versus P_0 are shown in Fig. 2(a), where it is seen that when $P_0 = 0.884$, 0.623, 0.468, 0.342, 0.260, 0.175, 0.158, 0.141 and 0.088, the theoretical velocities are in quantitative agreement with the experimental ones for the WT, 0P, 2P, 4P, 6P, 13P, 19P, 26P and 14GS motors, respectively. Then, with the above parameter values the theoretical results for the ATPase rate and chemomechanical coupling ratio for the WT and engineered motors are also consistent with the experimental data[21] (Figs. 2(b) and 2(c)). With the above parameter values, and by additionally taking $k_{\rm d} = 6.3\ {\rm s}^{-1}$ (Table 1), the theoretical results for the run length for the WT and engineered motors are also consistent with the experimental data[21] (Fig. 2(d)). Furthermore, with the results for the velocity (Fig. 2(a)) and those for the attachment duration (Fig. 2(e)), the obtained relationship between velocity and attachment duration is also in good agreement with that obtained from the experimental data[21] (Fig. 2(f)). In a word, with only three adjustable parameters, $k^{(+)}$, $k_{\rm d}$ and P_0, all the theoretical results for the WT and engineered motors are in quantitative agreement with the available experimental data[21] (Figs. 2(a)–2(d) and 2(f)).

Table 1. Parameter values for human kinesin-1 under the experimental conditions of Yildiz *et al.*[21] and for bovine brain kinesin-1 at temperature $T = 298$ K (25 °C) under the experimental conditions of Nara and Ishiwata.[25] Values with an asterisk are identical to those used before.[27]

Parameter	Human kinesin	Bovine brain kinesin
$k^{(+)}$ (${\rm s}^{-1}$)	62	80
$k^{(-)}$ (${\rm s}^{-1}$)	3.6*	3.6*
$k_{\rm D}$ (${\rm s}^{-1}$)	300*	300*
$k_{\rm NL}$ (${\rm s}^{-1}$)	1500*	1500*
E_0 ($k_{\rm B}T$)	3.6*	3.6*
$k_{\rm d}$ (${\rm s}^{-1}$)	6.3	16.2
$\varepsilon_{\rm s}$ (${\rm s}^{-1}$)	0.01	0

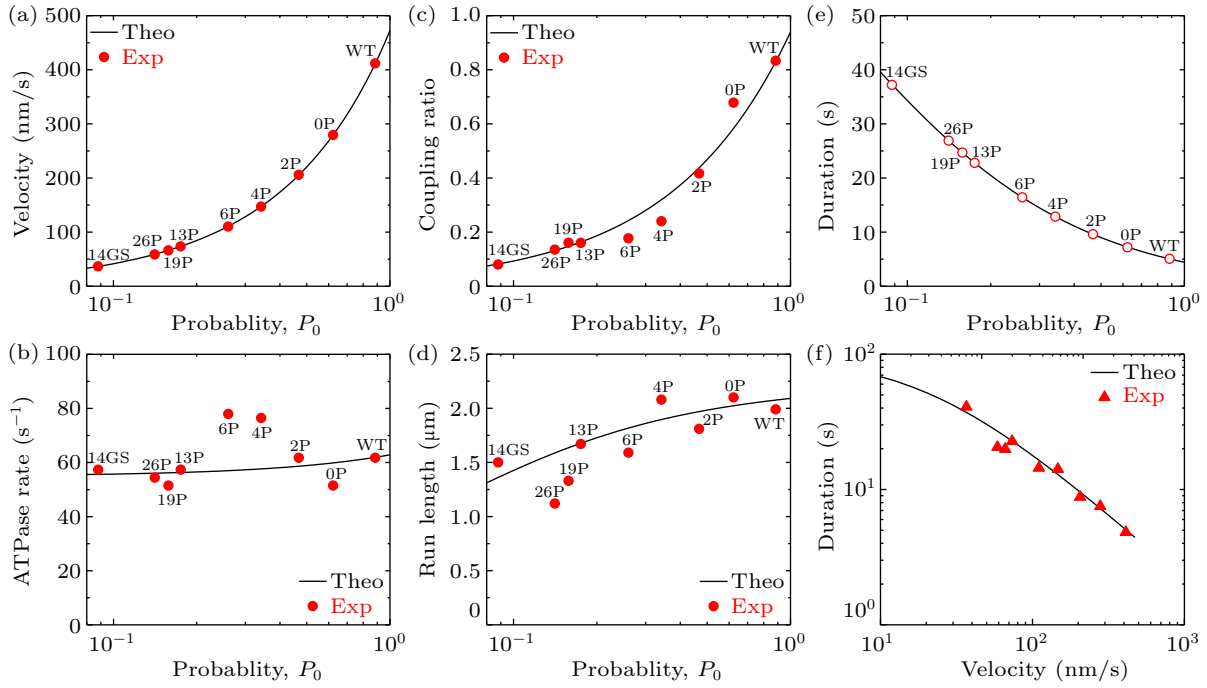


Fig. 2. Effect of varying intramolecular strain on the dynamics of human kinesin-1 at saturating ATP concentrations. Lines are theoretical results, filled symbols are experimental data from Yildiz *et al.*[21] and open symbols are predicted data, with WT, 0P, 2P, 4P, 6P, 13P, 19P, 26P and 14GS motors corresponding to $P_0 = 0.884$, 0.623, 0.468, 0.342, 0.260, 0.175, 0.158, 0.141 and 0.088, respectively: (a) velocity versus P_0; (b) ATPase rate versus P_0; (c) chemomechanical coupling ratio versus P_0; (d) run length versus P_0; (e) attachment duration versus P_0; (f) relationship between velocity and attachment duration.

The origin of the tradeoff between velocity and attachment duration (Fig. 2(f)) can be briefly explained as follows. As noted from Fig. 2(b) and Fig. S1 (see supplementary information), the ATPase rate of the motor, k, the ATPase rate of the trailing head, $k_{\rm T}$, and the ATPase rate of the leading head, $k_{\rm L}$, are insensitive to the variation of P_0. Since $P_{\rm E}$ is independent of P_0 (see Eq. (1)), from Eq. (5) it is noted that the velocity is approximately proportional to P_0. From Eqs. (7)–(9) it is noted that the detachment rate of the motor, which arises from detachment occurring in the weak MT-binding periods, $\varepsilon_{\rm w}$, is also approximately proportional to P_0. Since the total detachment rate of the motor, ε, is determined mainly by $\varepsilon_{\rm w}$ because $\varepsilon_{\rm s} \ll \varepsilon_{\rm w}$, the attachment duration of the motor is approximately inversely proportional to P_0. Therefore, with increase in P_0, the velocity decreases whereas the attachment duration increases, implying a tradeoff between velocity and attachment duration.

3.2. Effect of varying temperature

In this section, we study the effect of varying the solution temperature on the dynamics of a bovine brain kinesin motor at saturating ATP concentrations. The dependence of the rate constants of the ATPase activity on absolute temperature T can be calculated using the transition state theory formula[31–34]

$$k^{(+)} = k_0 \exp\left(-\frac{E_{\rm a}^{(+)}}{k_{\rm B}T}\right), \tag{13}$$

$$k^{(-)} = k_0 \exp\left(-\frac{E_{\rm a}^{(-)}}{k_{\rm B}T}\right), \tag{14}$$

$$k_{\rm D} = k_0 \exp\left(-\frac{E_{\rm a}^{(\rm D)}}{k_{\rm B}T}\right), \tag{15}$$

$$k_{\rm NL} = k_0 \exp\left(-\frac{E_{\rm a}^{(\rm NL)}}{k_{\rm B}T}\right), \tag{16}$$

where k_0 is a universal constant that is equivalent to the rate constant with zero activation energy, $E_{\rm a}^{(+)}$ is the activation energy of ATP transition to ADP in the kinesin head with its NL in forward orientation, $E_{\rm a}^{(-)}$ is the activation energy of ATP transition to ADP in the kinesin head with its NL not in forward orientation, $E_{\rm a}^{(\rm D)}$ is the activation energy of ADP release from the MT-bound head, and $E_{\rm a}^{(\rm NL)}$ is the activation energy of NL docking. As determined in the literature, the universal constant $k_0 \approx 6\times10^{12}$ s^{-1},[31–34] and thus in this work we take $k_0 = 6\times10^{12}$ s^{-1}.

The detachment of the motor from MT during the weak MT-binding period can be considered as a Brownian particle escaping from a potential well of depth $E_{\rm w2}$. For $E_{\rm w2} \gg k_{\rm B}T$, the dependence of the detachment rate during the weak MT-binding period, $k_{\rm d}$, on absolute temperature T can be approximately written as[35]

$$k_{\rm d} = k_{\rm d0}\frac{298}{T}\exp\left(-\frac{E_{\rm w2}}{k_{\rm B}T}\right), \tag{17}$$

where $k_{\rm d0}$ is the detachment rate with $E_{\rm w2} = 0$ at $T = 298$ K (25 °C). It should be mentioned that in Eq. (17), for approximation, we have not considered the variation of the solution viscosity and of affinity $E_{\rm w2}$ with T in the range of 293 K (20 °C) and 313 K (40 °C) studied in this work. Under a zero energy barrier, detachment of the kinesin motor from MT is equivalent to the free diffusion of a Brownian particle with a size of about 6 nm in a solution with a reflecting boundary, with the detachment time $t_{\rm d0}$ being of the order of 1 μs. Thus, the detachment rate $k_{\rm d0} = 1/t_{\rm d0}$ is about 10^6 s^{-1}.

In this section, we focus on the WT bovine brain kinesin motor. Since for the WT case P_0 approaches 1, for simplicity we take $P_0 = 1$ here. Since $\varepsilon_{\rm s}$ is very small and at saturating ATP the time of a chemomechanical coupling cycle is short, for approximation we can neglect the detachment of the motor in a chemomechanical coupling cycle during the strong MT-binding period and thus take $\varepsilon_{\rm s} = 0$ (Table 1) (see next section). Then, from Eqs. (1)–(12) it is seen that to study theoretically the dynamics of the WT bovine brain kinesin motor, values for the remaining parameters $k^{(+)}$, $k^{(-)}$, $k_{\rm D}$, $k_{\rm NL}$, E_0 and $k_{\rm d}$ are required. As in the previous section, here we also take $k^{(-)} = 3.6$ s^{-1}, $k_{\rm D} = 300$ s^{-1}, $k_{\rm NL} = 1500$ s^{-1} and $E_0 = 3.6k_{\rm B}T = 14.8$ pN·nm at $T = 298$ K (25 °C) for bovine brain kinesin (Table 1). The remaining two parameters $k^{(+)}$ and $k_{\rm d}$ are adjustable here to make the theoretical results consistent with the experimental data of Nara and Ishiwata.[25] At $T = 298$ K (25 °C), by taking $k^{(+)} = 80$ s^{-1} and $k_{\rm d} = 16.2$ s^{-1} (Table 1) the theoretical results of the velocity, attachment duration and run length are close to the experimental data.[25]

With the above values of $k^{(+)} = 80$ s^{-1}, $k^{(-)} = 3.6$ s^{-1}, $k_{\rm D} = 300$ s^{-1} and $k_{\rm NL} = 1500$ s^{-1} at $T = 298$ K (25 °C) (Table 1), using Eqs. (13)–(16) we obtain $E_{\rm a}^{(+)} = 102.98$ pN·nm, $E_{\rm a}^{(-)} = 115.73$ pN·nm, $E_{\rm a}^{(\rm D)} = 97.54$ pN·nm and $E_{\rm a}^{(\rm NL)} = 90.92$ pN·nm. With these values of $E_{\rm a}^{(+)}$, $E_{\rm a}^{(-)}$, $E_{\rm a}^{(\rm D)}$ and $E_{\rm a}^{(\rm NL)}$, the dependences of $k^{(+)}$, $k^{(-)}$, $k_{\rm D}$ and $k_{\rm NL}$ on T can be calculated with Eqs. (13)–(16). The dependence of $P_{\rm E}$ on T can be calculated with Eq. (1), where $E_0 = 14.8$ pN·nm (see above). With the above value of $k_{\rm d} = 16.2$ s^{-1} at $T = 298$ K (25 °C) (Table 1), using Eq. (17) the calculated results for the relationship between $k_{\rm d0}$ and $E_{\rm w2}$ are shown in Fig. 3(a). Thus, for a given $k_{\rm d0}$, which determines $E_{\rm w2}$ from Fig. 3(a), the dependence of $k_{\rm d}$ on T can be calculated with Eq. (17). As mentioned above, $k_{\rm d0}$ is about 10^6 s^{-1}. Thus, we take $k_{\rm d0} = 10^6$ s^{-1} here. The theoretical results for the velocity, attachment duration and run length versus T are shown in Figs. 3(b)–3(d). It is interesting that without any adjustable parameters here the theoretical results are in quantitative agreement with the experimental data of Nara and Ishiwata.[25] The predicted results

of the chemomechanical coupling ratio versus T are shown in Fig. 3(e), with the ratio being kept nearly equal to one. Furthermore, with the results for the velocity (Fig. 3(b)) and those for the attachment duration (Fig. 3(c)), the obtained relationship between the velocity and attachment duration is also in good agreement with that obtained from the experimental data[25] (Fig. 3(f)). In a word, with only two adjustable parameters $k^{(+)}$ and $k_{\rm d}$ to reproduce the experimental data for velocity, attachment duration and run length for one temperature, without any other adjustable parameters, all the theoretical results for other temperatures are in quantitative agreement with the available experimental data[25] (Figs. 3(b)–3(d) and 3(f)).

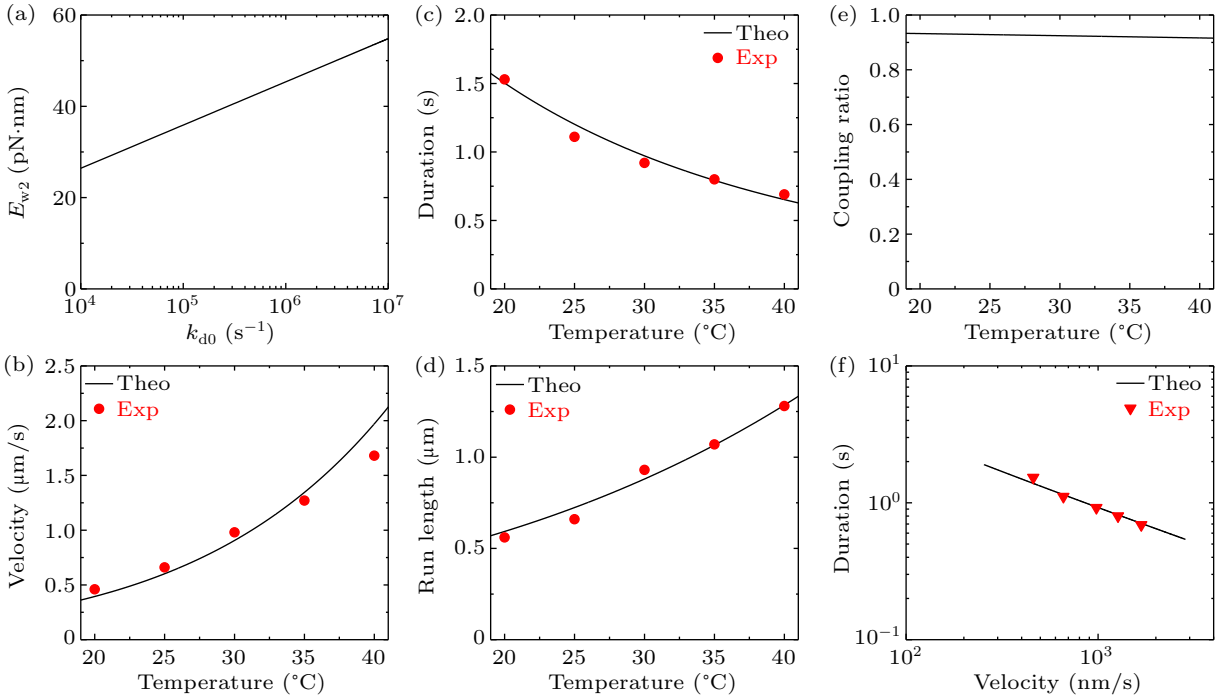


Fig. 3. Effect of varying solution temperature on the dynamics of bovine brain kinesin-1 at saturating ATP concentrations. Lines are theoretical results and symbols are experimental data from Nara and Ishiwata:[25] (a) the relationship between k_{d0} and E_{w2}, which gives the detachment rate during the weak MT-binding period, $k_{\rm d} = 16.2\ {\rm s}^{-1}$, at temperature $T = 298$ K (25 °C); (b) velocity versus temperature; (c) attachment duration versus temperature; (d) run length versus temperature; (e) chemomechanical coupling ratio versus temperature; (f) relationship between velocity and attachment duration.

The origin of the tradeoff between velocity and attachment duration (Fig. 3(f)) can be briefly explained as follows. From Eq. (5) we have $v = [P_{\rm E}k_{\rm T} - (1-P_{\rm E})k_{\rm L}]d$ for the WT bovine brain kinesin motor with $P_0 = 1$. From Eq. (1), it is noted that due to $P_{\rm E}$ approaching 1, $P_{\rm E}$ is insensitive to T (see Fig. S2(a) in the supplementary information). From Eqs. (2), (3) and (13)–(16), it is noted that $k_{\rm T}$ and $k_{\rm L}$ increase approximately exponentially with T (see Figs. S2(b) and S2(c) in the supplementary information). Thus, the velocity v increases approximately exponentially with T (Fig. 3(b)). Due to $k_{\rm d}$ being much smaller than $k_{\rm D}$ and E_{w2} being smaller than $E_{\rm a}^{\rm (D)}$, from Eqs. (7) and (8) it is noted that $P_{\rm w}P_{\rm d}$ decreases approximately exponentially with T (Fig. S2(d) in supplementary information). By comparing Figs. S2(b) and S2(c) with Fig. S2(d), it is seen that the magnitude of the increasing slope of $\log(k_{\rm T}+k_{\rm L})$ versus $\log(T)$ is larger than the magnitude of the decreasing slope of $\log(P_{\rm w}P_{\rm d})$ versus $\log(T)$. Thus, from Eq. (9) it is expected that $\varepsilon_{\rm w}$ will increase approximately exponentially with T, which leads to the attachment duration decreasing approximately exponentially with T (Fig. 3(c)). Consequently, with increase in T, the velocity increases whereas the attachment duration decreases, implying a tradeoff between the two factors.

3.3. Effect of varying the ATP concentration

In this section, we study the effect of varying the ATP concentration on the dynamics of a bovine brain kinesin motor at fixed temperature $T = 298$ K (25 °C). As above, for the WT motor we take $P_0 = 1$. As derived before (see supplementary information in Ref. [29]), at non-saturating ATP concentrations the average ATPase rates of the trailing and leading heads can be approximately written as

$$k_{\rm T} = P_{\rm E}\left(\frac{1}{k^{(+)}} + \frac{1}{k_{\rm b}[{\rm ATP}]} + \frac{1}{k_{\rm NL}}\right)^{-1} + (1-P_{\rm E})\left(\frac{1}{k_{\rm D}} + \frac{1}{k_{\rm b}[{\rm ATP}]} + \frac{1}{k^{(+)}} + \frac{1}{k_{\rm NL}}\right)^{-1}, \quad (18)$$

$$k_{\rm L} = P_{\rm E}\left(\frac{1}{k_{\rm D}} + \frac{1}{k^{(-)}} + \frac{1}{k_{\rm b}[{\rm ATP}]} + \frac{k_{-1}}{k_{\rm b}[{\rm ATP}]k^{(-)}}\right)^{-1} + (1-P_{\rm E})\left(\frac{1}{k^{(-)}} + \frac{1}{k_{\rm b}[{\rm ATP}]} + \frac{k_{-1}}{k_{\rm b}[{\rm ATP}]k^{(-)}}\right)^{-1}, \quad (19)$$

where k_b is the second-order rate constant of ATP binding to the nucleotide-free head, k_{-1} is the rate of ATP release from the head with an open nucleotide-binding pocket (i.e., the leading head) and the rate of ATP release from the head with a closed nucleotide-binding pocket (i.e., the trailing head) is implicitly taken to be zero. At non-saturating ATP concentrations, but with the equations for k_T and k_L being replaced by Eqs. (18) and (19), all other equations are the same as those presented in Section 2.

Here, we consider two values for ε_s, with $\varepsilon_s = 0$ and $\varepsilon_s = 0.01\ s^{-1}$. As done before (see supplementary information in Ref. [29]), we take $k_b = 2\ \mu M^{-1}\cdot s^{-1}$ and $k_{-1} = 80\ s^{-1}$ here. All other parameter values for the bovine brain kinesin motor are listed in Table 1. In Figs. 4(a)–4(e), we show the theoretical results of the velocity, ATPase rate, chemomechanical coupling ratio, run length and attachment duration versus ATP concentration. Furthermore, with the results for velocity (Fig. 4(a)) and those for attachment duration (Fig. 4(e)), the obtained relationship between velocity and attachment duration is shown in Fig. 4(f). From Fig. 4(c) it is seen that with change in the ATP concentration the chemomechanical coupling ratio is kept nearly equal to 1, which is in agreement with the available experimental data.[15,16] This feature of the chemomechanical coupling ratio (Fig. 4(c)) is similar to that for a change of solution temperature (Fig. 3(e)) but contrasts with that for a change in intramolecular strain (Fig. 2(c)). Thus, for varying ATP concentration, as for varying solution temperature, the increase in velocity arises mainly from an increase in the ATPase rate. From Fig. 4(e) it is seen that the attachment duration decreases with increase in the ATP concentration. The increase of velocity with increase in ATP concentration (Fig. 4(a)) and the decrease of attachment duration with increase in ATP concentration (Fig. 4(e)) result in the run length being nearly independent of ATP concentration when $\varepsilon_s = 0$ and the run length at very low ATP concentrations (e.g., 2 μM) being smaller than at saturating ATP concentrations (e.g., 2 mM) when $\varepsilon_s = 0.01\ s^{-1}$ (Fig. 4(d)). In addition, from Figs. 4(d) and 4(e) it is seen that at saturating ATP the effect of ε_s on the dynamics of the motor is very small and thus can be neglected, as done above. From Fig. 4(f) it is seen that a tradeoff between velocity and attachment duration is also present for varying ATP concentration.

The origin of the tradeoff (Fig. 4(f)) can be briefly explained as follows. From Eq. (1) it is seen that P_E is independent of ATP concentration. Thus, from $v = [P_E k_T - (1-P_E)k_L]d$ for a WT bovine brain kinesin motor with $P_0 = 1$ (Eq. (5)) the velocity is proportional to k_T and k_L. From Eqs. (18) and (19), it is noted that k_T and k_L increase with ATP concentration. Thus, the velocity increases with ATP concentration (Fig. 4(a)). From Eqs. (7)–(9), it is noted that ε_w increases linearly with increase in $k_T + k_L$. Thus, the total detachment rate ε, which is determined mainly by ε_w, increases with ATP concentration. Therefore, with increase in the ATP concentration, the velocity increases whereas the attachment duration decreases, implying a tradeoff between velocity and attachment duration.

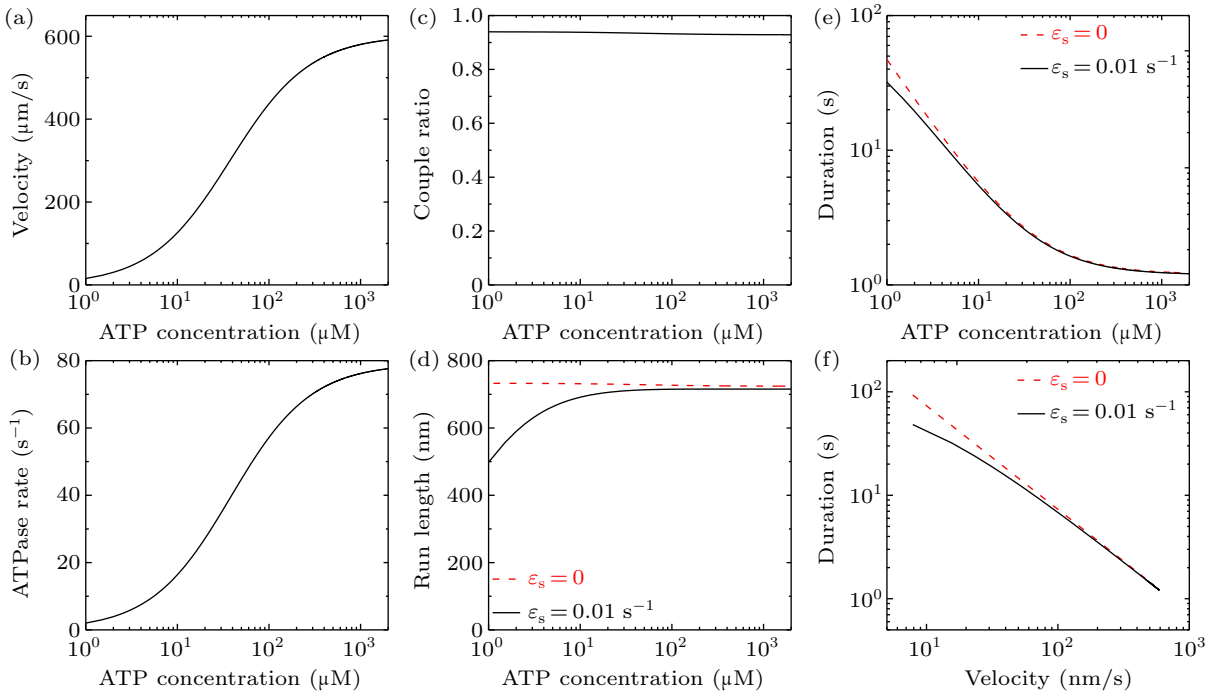


Fig. 4. Effect of varying ATP concentration on the dynamics of bovine brain kinesin-1 at temperature $T = 298$ K (25 °C). (a) Velocity versus ATP concentration: the velocity is independent of ε_s. (b) ATPase rate versus ATP concentration: the ATPase rate is independent of ε_s. (c) Chemomechanical coupling ratio versus ATP concentration: the ratio is independent of ε_s. (d) Run length versus ATP concentration for $\varepsilon_s = 0$ and $\varepsilon_s = 0.01\ s^{-1}$. (e) Attachment duration versus ATP concentration for $\varepsilon_s = 0$ and $\varepsilon_s = 0.01\ s^{-1}$. (f) Relationship between velocity and attachment duration for $\varepsilon_s = 0$ and $\varepsilon_s = 0.01\ s^{-1}$.

3.4. Effect of varying the rate of ATP transition to ADP

In this section, we study the effect of varying the rate of ATP transition to ADP on the dynamics of a bovine brain kinesin motor at saturating ATP and at fixed temperature $T = 298$ K (25 °C). In experiments, this can be realized by mutating residues near the nucleotide-binding pocket. For simplicity, we consider that the mutation has little effect on the rate of ADP release. For the mutated case, the rates of ATP transition to ADP in heads with and without forward NL orientation, $k^{(+)}$ and $k^{(-)}$, are taken to be multiplied by a factor α ($\alpha \leq 1$) relative to the WT case, while all other parameters are the same as for the WT case. In other words, except for $k^{(+)}$ and $k^{(-)}$ being replaced by $\alpha k^{(+)}$ and $\alpha k^{(-)}$, respectively, all equations are the same as those given in Section 2.

As above, for the WT motor we take $P_0 = 1$ here and consider two values for ε_s, namely $\varepsilon_s = 0$ and $\varepsilon_s = 0.01$ s^{-1}. All other parameters for the bovine brain kinesin motor are listed in Table 1. In Figs. 5(a)–5(e) we show the theoretical results for the velocity, ATPase rate, chemomechanical coupling ratio, run length and attachment duration versus α. As expected, the ATPase rate, and thus the velocity, increase approximately linearly with increase in α (Figs. 5(a) and 5(b)), giving a chemomechanical coupling ratio that is nearly independent of α (Fig. 5(c)). Interestingly, with increase in α the attachment duration decreases faster than linearly (Fig. 5(e)), resulting in the run length decreasing faster than linearly (Fig. 5(d)). We can explain the origin of these features as follows. Since $P_0 = 1$, P_E is nearly equal to 1, $k_{NL} \gg k^{(+)}$ and $k^{(-)} \ll k^{(+)}$, and from Eqs. (2)–(5) it is noted that k_T, k_L, k and v increase approximately linearly with increase in α. Since $k_D \gg k^{(+)}$ and $k_D \gg k_d$, from Eqs. (7) and (8) it is noted that $P_w P_d$ increases approximately linearly with increase in α. As already mentioned, k_T and k_L increase approximately linearly with increase in α. Thus, from Eq. (9) we note that with the increase in α, ε_w increases faster than linearly, resulting in the attachment duration decreasing faster than linearly. Furthermore, with the results for velocity (Fig. 5(a)) and those for attachment duration (Fig. 5(e)), the obtained relationship between velocity and attachment duration is plotted in Fig. 5(f), showing the tradeoff between the two factors.

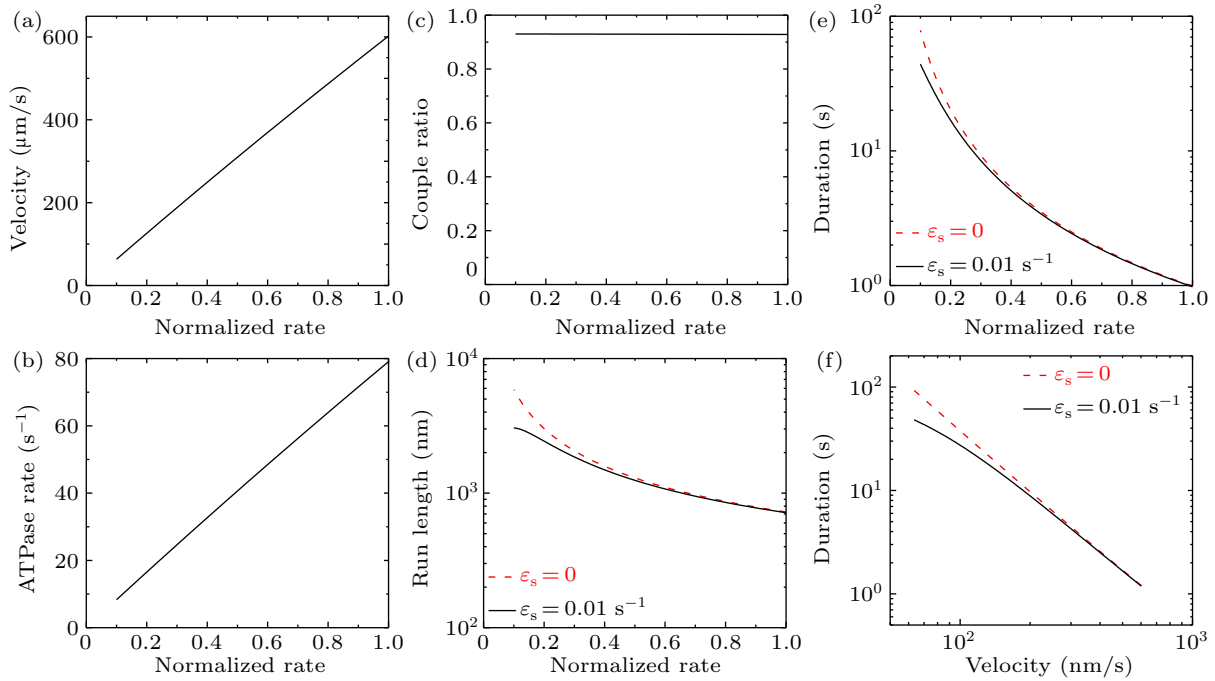


Fig. 5. Effect of varying the rate of ATP transition to ADP on the dynamics of bovine brain kinesin-1 at temperature $T = 298$ K (25 °C) and at saturating ATP concentrations. The normalized rate of ATP transition to ADP is defined as the rate for the motor with mutation of residues near the nucleotide-binding pocket normalized by that for the WT motor. (a) Velocity versus normalized rate of ATP transition to ADP: the velocity is independent of ε_s. (b) ATPase rate versus normalized rate of ATP transition to ADP: the ATPase rate is independent of ε_s. (c) Chemomechanical coupling ratio versus normalized rate of ATP transition to ADP: the ratio is independent of ε_s. (d) Run length versus normalized rate of ATP transition to ADP for $\varepsilon_s = 0$ and $\varepsilon_s = 0.01$ s^{-1}. (e) Attachment duration versus normalized rate of ATP transition to ADP for $\varepsilon_s = 0$ and $\varepsilon_s = 0.01$ s^{-1}. (f) Relationship between velocity and attachment duration for $\varepsilon_s = 0$ and $\varepsilon_s = 0.01$ s^{-1}.

3.5. Comparison of the relationship between velocity and attachment duration for different cases

In Figs. 2(f), 3(f), 4(f) and 5(f) we show the relationship between the velocity and attachment duration for four different cases. To make a clearer comparison, we summarize these relationships in Fig. 6 (solid lines), where the available experimental data[21,25] are also shown (triangles). In Fig. 6, curve 1 (red solid line) corresponds to the curve shown in Fig. 2(f) for the case of varying intramolecular strain, curve 2 (blue solid line) corresponds to the curve shown in Fig. 3(f) for the case of varying solution temperature, curve 3 (black solid line) corresponds to the solid curve shown in Fig. 4(f) for the case of

varying ATP concentration and curve 4 (green solid line) corresponds to the solid curve shown in Fig. 5(f) for the case of varying the rate of ATP transition to ADP.

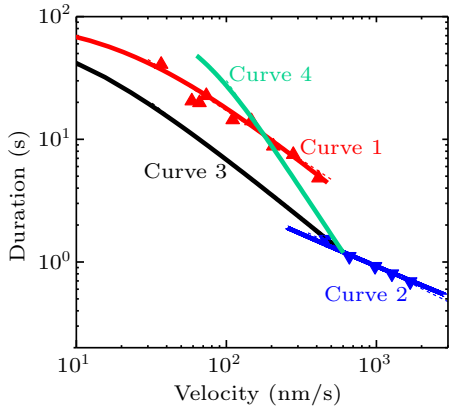


Fig. 6. Relationships between velocity and attachment duration under four different cases. Curve 1 (red solid line) corresponds to the curve shown in Fig. 2(f) for the case of varying intramolecular strain, with the red triangles being the experimental data from Yildiz *et al.*[21] Curve 2 (blue solid line) corresponds to the curve shown in Fig. 3(f) for varying solution temperature, with the blue triangles being the experimental data from Nara and Ishiwata.[25] Curve 3 (black solid line) corresponds to the solid curve shown in Fig. 4(f) for varying ATP concentration. Curve 4 (green solid line) corresponds to the solid curve shown in Fig. 5(f) for varying the rate of ATP transition to ADP. Thin dashed lines are the power law ($T_a \propto v^{-\alpha}$) fitting to the solid curves in the region of larger v or to the experimental data if they are present, with $\alpha = 0.8$, 0.6, 0.95 and 1.8 for curves 1, 2, 3 and 4, respectively.

By comparing curve 2 with curve 1, it is interesting that for varying solution temperature the attachment duration decreases more slowly with velocity than for varying intramolecular strain. This can be explained as follows. For varying solution temperature (see Subsection 3.2), since $\log(P_w P_d)$ decreases with $\log(T)$ (Fig. S2(d)) it is expected that the magnitude of the increasing slope of $\log(v)$ versus $\log(T)$ is larger than that of $\log(\varepsilon_w)$ versus $\log(T)$, resulting in the magnitude of the increasing slope of $\log(v)$ versus $\log(T)$ being larger than the magnitude of the decreasing slope of $\log(T_a)$ versus $\log(T)$. By comparison, for varying intramolecular strain (see Subsection 3.1), the magnitude of the increasing slope of $\log(v)$ versus $\log(P_0)$ is nearly equal to that of $\log(\varepsilon_w)$ versus $\log(P_0)$. Thus, for varying solution temperature the attachment duration would decrease more slowly with velocity than when intramolecular strain is varied.

By comparing curve 3 with curve 1, it is seen that for varying ATP concentration and varying intramolecular strain we have similar rates of decrease of attachment duration versus velocity. This can be explained as follows. For varying ATP concentration (see Subsection 3.3), the velocity is proportional to k_T and k_L, and ε_w is also proportional to k_T and k_L, with k_T and k_L increasing with ATP concentration. For varying intramolecular strain (see Subsection 3.1), the velocity is approximately proportional to P_0, and ε_w is also approximately proportional to P_0. The slight difference in the rate of decrease of attachment duration versus velocity between the two cases can be explained as follows. For varying ATP concentration, the change in velocity arises from the change in the ATPase rate whereas the chemomechanical coupling ratio is virtually unchanged (Fig. 4). By contrast, for varying intramolecular strain, the change in velocity arises from the change in the chemomechanical coupling ratio whereas the ATPase rate is virtually unchanged (Fig. 2).

By comparing curve 4 with curve 3, it is seen that for varying rate of ATP transition to ADP the attachment duration decreases faster with velocity than when ATP concentration is varied. This can be explained as follows. For varying rate of ATP transition to ADP (see Subsection 3.4), with increase in α the velocity increases approximately linearly (Fig. 5(a)) whereas the attachment duration decreases faster than linearly (Fig. 5(e)). By comparison, for varying ATP concentration (see Subsection 3.3), the velocity is proportional to k_T and k_L, and ε_w is also proportional to k_T and k_L, with k_T and k_L increasing with ATP concentration.

Similar to the work of Rizvi,[26] we fit the theoretical results (solid curves) in the region of larger v or fit the experimental data if they are present using the power-law relation $T_a \propto v^{-\alpha}$ (thin dashed lines), with $\alpha = 0.8$, 0.6, 0.95 and 1.8 for curves 1, 2, 3 and 4, respectively. Note that $\alpha = 0.8$ for curve 1 under the case of varying intramolecular strain and $\alpha = 0.6$ for curve 2 under the case of varying temperature are the same as the values obtained in Ref. [26]. Interestingly, it is seen that for a varying rate of ATP transition to ADP (curve 4) α has the largest value of 1.8, which is the same as that obtained in Ref. [26] by fitting the experimental data of Cleary *et al.*[36] for a dynein motor (see Fig. S3 in the supplementary information). Note that the experimental data of Cleary *et al.*[36] for a dynein motor were obtained by mutating residues that affect the ATPase activity, which is similar to the case of variation of the rate of ATP transition to ADP studied here for the kinesin motor. As shown by previous modeling studies, the cytoplasmic dynein dimer could have a similar chemomechanical coupling pathway to the kinesin dimer.[37] Thus, it is expected that $\alpha = 1.8$ obtained here for a kinesin motor should be consistent with that obtained by fitting the experimental data of Cleary *et al.*[36] to the theoretical equations for a dynein motor.

4. Concluding remarks

In this paper we have studied the dynamics of kinesin motors theoretically under four different cases, including varying intramolecular strain, solution temperature, ATP concentration and the rate of ATP transition to ADP that can be realized by mutating the residues near the nucleotide-binding pocket. The theoretical results explain quantitatively the available experimental data and provide predictions. The results show that

different cases can lead to different rates of decrease of the attachment duration versus velocity. The origin of the tradeoff between velocity and attachment duration is explained. The origin of the difference in the decreasing rate of attachment duration versus velocity for different cases is explained. Finally, it should be mentioned that this work only focuses on the case of no load on the motor. However, note that under a given load on the motor, the tradeoff between velocity and attachment duration for the four cases should be still maintained.

Acknowledgment

We are very grateful to Professor P Xie for the constructive discussions and comments on the manuscript.

References

[1] Vale R D, Reese T S and Sheetz M P 1985 *Cell* **42** 39
[2] Lawrence C J, Dawe R K, Christie K R, Cleveland D W, Dawson S C, Endow S A, Goldstein LSB, Goodson H V, Hirokawa N and Howard J 2004 *Cell Biol.* **167** 19
[3] Kozielski F, Sack S, Marx A, Thormählen M, Schönbrunn E, Biou V, Thompson A, Mandelkow E M and Mandelkow E 1997 *Cell* **91** 985
[4] Shang Z, Zhou K, Xu C, Csencsits R, Cochran J C and Sindelar C V 2014 *eLife* **3** e04686
[5] Howard J 1996 *Annu. Rev. Physiol.* **58** 703
[6] Asbury C L 2005 *Curr. Opin. Cell Biol.* **17** 89
[7] Block S M 2007 *Biophys. J.* **92** 2986
[8] Cross R A 2017 *Biopolymers* **105** 476
[9] Xie P 2021 *Commun. Theor. Phys.* **73** 057601
[10] Xie P 2023 *J. Biol. Phys.* **49** 77
[11] Xie P 2023 *Biophysica* **3** 46
[12] Vale R D 2003 *Cell* **112** 467
[13] Asbury C L, Fehr A N and Block S M 2003 *Science* **302** 2130
[14] Yildiz A, Tomishige M, Vale R D and Selvin P R 2004 *Science* **303** 676
[15] Block S M, Goldstein L S and Schnapp B J 1990 *Nature* **348** 348
[16] Svoboda K, Schmidt C F, Schnapp B J and Block S M 1993 *Nature* **365** 721
[17] Hua W, Young E C, Fleming M L and Gelles J 1997 *Nature* **388** 390
[18] Coy D L, Wagenbach M and Howard J 1999 *J. Biol. Chem.* **274** 3667
[19] Kaseda K, Higuchi H and Horose K 2002 *Proc. Natl. Acad. Sci. USA* **99** 16058
[20] Clancy B E, Behnke-Parks W M, Andreasson J O L, Rosenfeld S S and Block S M 2011 *Nat. Struct. Mol. Biol.* **18** 1020
[21] Yildiz A, Tomishige M, Gennerich A and Vale R D 2008 *Cell* **134** 1030
[22] Taniguchi Y, Nishiyama M, Ishii Y and Yanagida T 2005 *Nat. Chem. Biol.* **1** 342
[23] Kawaguchi K and Ishiwata S 2000 *Biochem. Biophys. Res. Commun.* **272** 895
[24] Kawaguchi K and Ishiwata S 2001 *Cell Motility and the Cytoskeleton* **49** 41
[25] Nara I and Ishiwata S 2006 *Biophysics* **2** 13
[26] Rizvi M S 2022 *J. Biol. Phys.* **48** 369
[27] Xie P 2021 *J. Theor. Biol.* **530** 110879
[28] Xie P 2023 *J. Theor. Biol.* **571** 111556
[29] Xie P 2020 *ACS Omega* **5** 5721
[30] Guo S K, Wang P Y and Xie P 2017 *J. Theor. Biol.* **414** 62
[31] Glennon T M, Villa J and Warshel A 2000 *Biochemistry* **39** 9641
[32] Grigorenko B L, Rogov A V, Topol I A, Burt S K, Martinez H M and Nemukhin A V 2007 *Proc. Natl. Acad. Sci. USA* **104** 7057
[33] Xie P 2019 *Cell Mol. Bioeng.* **12** 179
[34] Xie P, Guo S K and Chen H 2019 *Int. J. Mol. Sci.* **20** 4911
[35] Xie P 2009 *J. Theor. Biol.* **259** 434
[36] Cleary F B, Dewitt M A, Bilyard T, Htet Z M, Belyy V, Chan D D, Chang A Y and Yildiz A 2014 *Nat. Commun.* **5** 4587
[37] Xie P 2019 *Euro. Biophys. J.* **48** 609